SPLITTING OF LIGHT BEAMS WITH PHASE DISLOCATIONS INTO SOLITONS IN QUADRATIC NONLINEAR MEDIA

ROTURA DE HACES ÓPTICOS CON DISLOCACIONES DE FASE Y FORMACIÓN DE SOLITONES EN MEDIOS NO LINEALES CUADRÁTICOS

Dmitri V. Petrov, Lluis Torner y Maria C. Santos*

Departamento de Teoría de la Señal y Comunicaciones, Universitat Politecnica de Catalunya, Gran Capitan UPC-D3, Barcelona, ES 08034, Spain

ABSTRACT

We investigate the propagation of intense light beams in bulk quadratic nonlinear crystals under conditions for second-harmonic generation. We show numerically that input light beams with a spiral phase front dislocation self-split in the crystal into several spatial solitons. For input fundamental and its second harmonic gaussian beams the latter with a phase dislocation, the number and pattern of output solitons can be controlled by the material and wave parameters involved, and in particular by the input light intensity and by the topological charge of the dislocation. In second harmonic generation processes with a phase dislocation in the input fundamental beam the output pattern of the solitons may be controlled by a low-intensity double frequency gaussian beam.

Key words: Vortices, cascading, splitting, soliton, quadratic nonlinear.

RESUMEN

En este artículo se investiga la propagación de haces de luz intensos en medios homogéneos con respuesta no lineal cuadrática, bajo condiciones de generación del segundo armónico. Se muestra numéricamente que haces de entrada con una dislocación en espiral del frente de onda se rompen en el medio no lineal para formar varios solitones espaciales. El número y características de los solitones a la salida cuando se inyectan haces gaussianos tanto a frecuencia fundamental como a su segundo armónico, este último con dislocación de fase, pueden controlarse mediante parámetros típicos del material y de las ondas que intervienen y en particular mediante la intensidad de la potencia de entrada y la carga topológica de la dislocación. Cuando la dislocación de fase es contenida en el haz fundamental, puede usarse como control un haz gaussiano de baja intensidad a frecuencia doble.

Palabras clave: Vórtices, cascading, rotura de haz, solitón, nolinealidad cuadrática.

* Dirección Permanente: Institute of Semiconductor Physics, Novosibirsk, 630090, Russia.

Recibido: 17-02-97

1. INTRODUCTION

Light propagation in quadratic nonlinear media exhibits a fascinating variety of phenomena [1], whose implications go far beyond conventional frequency conversion applications. One important example is the formation of spatial solitons (more properly, solitary waves) [2]. Solitons exist in a wide variety of material and input light conditions in both bulk crystals and planar waveguides [3,4], and they have been observed experimentally by Torruellas et. al. [5], and Schiek et. al [6].

Under conditions for second-harmonic generation, the solitons form by mutual trapping of the fundamental and second harmonic beams. The existence of these solitons along with their associated propagation dynamics hold promise for different applications, in particular for the realization of all-optical operations such as beam steering and scanning, and switching [7,8]. By and large, the principle of operation leading to such effects involves the control of the location of the output light beams that exit the quadratic material. Such control can be accomplished in a variety of ways by exploiting the mutual dragging of the two waves forming the solitons. In the geometries studied to date the key ingredient for soliton control is either the existence of Poynting vector beam walk-off between the fundamental and second harmonic beams, and/or the use of tilted input light beams that carry non-vanishing transverse momentum.

In this paper we explore the dynamical regime, in which the input light carries angular momentum associated with the field envelopes [9]. Our aim is to show that it offers new opportunities for the control of light by light. Naturally, there are many interesting situations and here we have selected two representative cases that capture many of the essential features and that hold promise for experimental demonstration.

Specifically, as a first case we consider the beam evolution in bulk crystals when both the fundamental and second harmonic input beams are Gaussian, but the second harmonic beam contains a vortex nested in its center. We show numerically that depending on the input light conditions, the beams either form a single soliton or they self-split into several solitons. We discuss the origin of the splitting and how the number of output solitons depends on the input light intensities and on the topological charge of the phase dislocation. We briefly study the effects introduced by a wavevector mismatch and the presence of Poynting vector walk-off.

The second case is second harmonic generation, i.e. the input consists only of a fundamental beam with a phase dislocation. In this case the process of second harmonic generation becomes unstable against azimuthal modulations. Numerical simulations were carried out for initial conditions including a small random noisy field for the study of this effect.

Usually beams with a phase dislocation are referred to as an optical vortices. Optical vortices and their associated dynamics in both linear and cubic nonlinear media have been investigated by several authors in the last few years [10-14], and they have been shown to display interesting properties with potential applications. In particular, Tikhonenko and co-workers observed experimentally the break-up of a modulationally unstable vortex into bright solitons in saturable self-focusing cubic nonlinear media [14], a phenomenon somehow similar to the splitting that we study here.

2. OPTICAL VORTEX: FIELD DISTRIBUTION AND METHODS OF GENERATION

An optical vortex is a spiral dislocation of the phase-front that has a helical phase-ramp around a phase singularity. Laguerre-Gaussian beams, which include a $\exp(im\varphi)$ azimuthal dependence in the field distribution are of special interest because they are rather easily generated experimentally. The field of a Laguerre-Gaussian beam propagating along the z-axis is given by

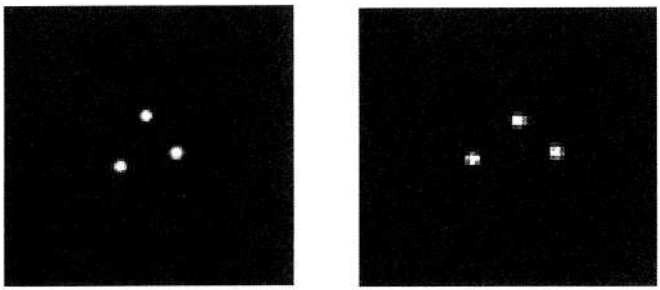

FIGURE 9. Fundamental beam after propagation up to ξ =10 by SHG with an initial amplitude and A = 6 for two realizations of the noise term.

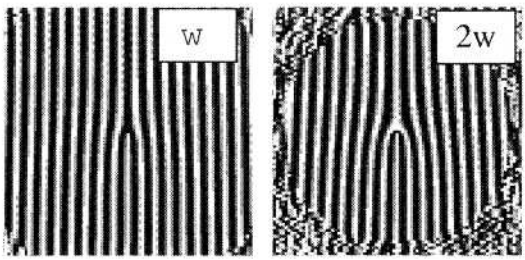

FIGURE 10. Interference fringes for the fundamental beam and double frequency beam in Figure 9.

where R is the random complex number sequence. The random sequence is assumed to have zero average, and a uniform distribution in the range [-1,1]. In our experiments we used a scale factor that gives a variance of 10^{-2}. The random sequence was generated by a standard pseudo-random number generator [19]. The noise simulates fluctuations in the input beam that always exist by experimental realization of the SHG and 'seeds' the azimuthal modulational instability.

We did numerical simulations for several realizations of the noise term. In all cases three soliton were observed at ξ =10 (Fig. 9). Notice that in this case we observed a generation of the topological defects $2m$ in the second harmonic field. (Fig. 10).

5. CONCLUSIONS

To summarize, we have shown numerically that focused light beams with a spiral phase dislocation propagating in bulk quadratic nonlinear crystals self-split into several spatial solitons. The self-splitting process occurs in a wide variety of conditions, including second-harmonic generation settings that involve ring-shaped input beams. Here we presented simple situations and discussed the fact that the number and pattern of output solitons can be controlled by the material and wave parameters involved, and in particular by the input light intensity and by the topological charge of the dislocation. The self-splitting process that we predict requires experimental features similar to the formation of single solitons [5,8], hence it holds promise for experimental demonstration.

This work has been supported by the Direccio General de Recerca de la Generalitat de Catalunya, by the Universitat Politecnica de Catalunya and by the Spanish Government under

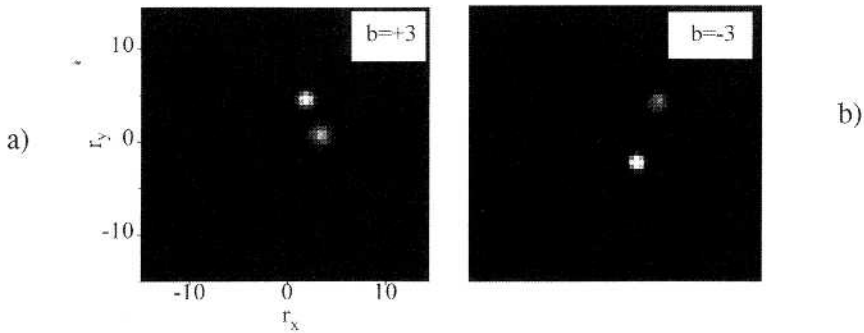

FIGURE 8. Same as in Fig. 3(b), but at positive and negative wavevector mismatch. (a): $\beta = 3$; (b): $\beta = -3$. In both cases $m = 1$, $A = 3$, $B = 4$, and $\delta = 0$.

raised from the Figures is that they clearly confirm the robustness of the self-splitting process, as it happens over a range of conditions producing a reasonably uniform output pattern. Thus, the effect holds promise for experimental exploration.

The dynamics and result of the beam splitting also depend on the material and linear wave propagation conditions, namely the wavevector mismatch and Poynting vector walk-off between the interacting beams, as so does the formation of solitons in the simpler case of cylindrically symmetric beams [3]. In particular, the soliton properties themselves, e.g. the fraction of power carried by each of the two waves forming the soliton, are different at positive and negative wavevector mismatch. All this impacts strongly the details of the beam splitting process and a comprehensive and detailed study shall be published in the future, but under appropriate input light conditions the number of output solitons is also given by the results obtained at phase-matching and described above. As a representative example, Fig. 8 shows the output solitons obtained at ß = ±3, for the same conditions as in Fig. 2(b).

Beam splitting into several solitons similar to the phenomenon that we predict here also occurs when only a fundamental beam with a variety of ring-like beam shapes, including phase dislocations nested in a Gaussian, higher-order Laguerre-Gaussian beams or general laser doughnut modes, are considered as the input light conditions. Notice that this is an important point from a practical point of view, because the experimental set-up required is simpler than the situation that we have reported here. In such case the beams self-split because of the azimuthal modulational instability of the flat top of the ring-shaped beams [17], a process similar to the break-up of analogous beams in saturable cubic nonlinear media [14,18]. Therefore, this process has both, a different interpretation and a different dynamics than the splitting that we studied here and thus requires a separate detailed investigation.

Next we consider the above situation, namely we assume that only a single-charged vortex beam at the fundamental frequency is launched into the crystal. In this case, the ring-shaped beams at both ϖ and 2ϖ are modulationally unstable, thus to 'seed' the instability we add a small, noisy field to the input conditions. We suppose that the noise induces both amplitude and phase fluctuations, so that the input field is

$$a_1(\xi = 0, r\perp) = Ar\perp \exp(i\varphi) \exp(-r_\perp^2/w^2)(1 + R)$$
$$a_2(r_{\perp x}, r_{\perp y}, \xi = 0) = 0 \qquad (10)$$

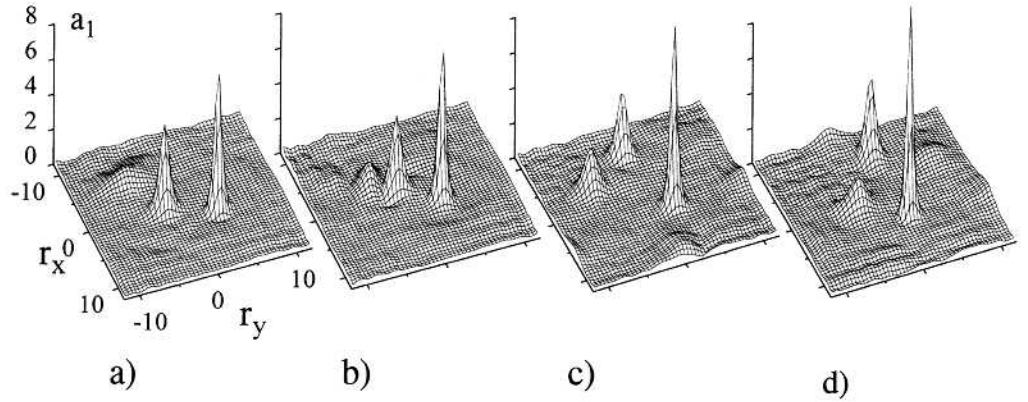

FIGURE 5. Same as in Fig. 5, but for different input conditions. Here, in all cases $m = 1$ and $B = 4$. In (a): $A = 2$, in (b): $A = 3$, in (c): $A = 4$, and in (d): $A = 5$.

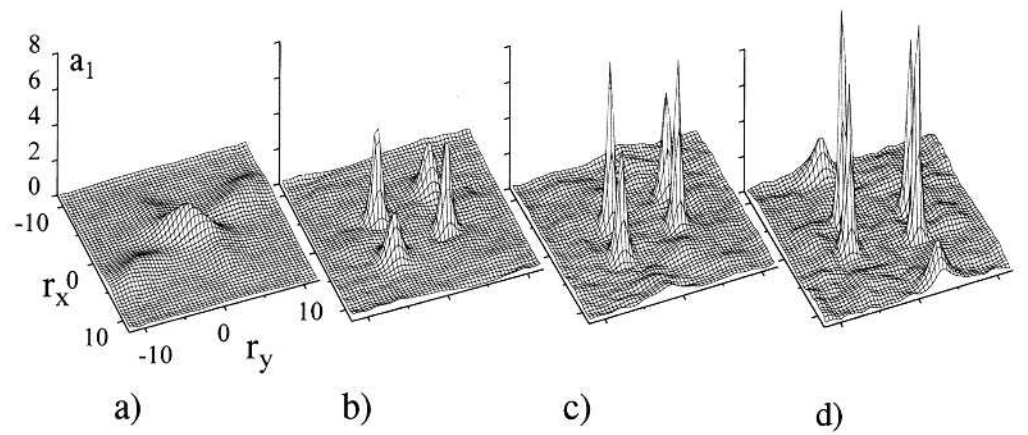

FIGURE 6. Same as in Fig. 5, but for different input conditions. Here, in all cases $m = 2$ and $A = 3$. In (a): $B = 1$, in (b): $B = 2$, in (c): $B = 3$, and in (d): $B = 4$.

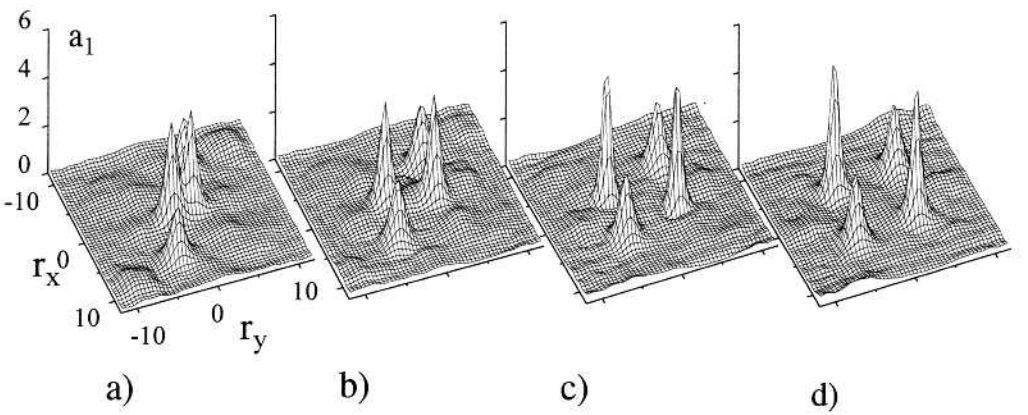

FIGURE 7. Same as in Fig. 5, but for different input conditions. Here, in all cases $m = 2$ and $B = 2$. In (a): $A = 1$, in (b): $A = 2$, in (c): $A = 3$, and in (d): $A = 4$.

they tend to be either radiated or transferred to the regions where a soliton is formed. Of course, the actual beam evolution in either of the above regions depends on the light intensity. The partition of the beam dynamics into separate azimuthal pieces is readily exposed by examining the initial rate of power exchange between two cylindrically symmetrical, but out-of-phase input beams. Writing the fields in the form $\alpha_1 = R_1(r\perp)$ and $a_2 = R_2(r\perp)\exp(i\phi_0)$, with $R_{1,2}$ and ϕ_0 being real quantities, one obtains

$$\left.\frac{dI_2}{d\xi}\right|_{\xi=0} = 2\int R_1^2 R_2 \sin(\phi_0) dr\perp. \tag{9}$$

By and large, in-phase input beams (i.e., having $\phi_0 = 0$) with similar amplitudes form solitons much more easier than inputs with a phase difference of π [3]. Thus, in the case that we study here in general solitons tend to form nearby the regions where the input beams are in-phase whereas the portions of the beams that experience a π initial phase difference tend to spread. Also, the beam evolution is not symmetric around $\phi_0 = 0$. In particular, according to (9), input beams with a positive phase difference, say $|\phi_0|$, start transferring power from the fundamental to the second harmonic, whereas input beams with the same phase difference but with a negative value, i.e. $-|\phi_0|$, start transferring power from the second harmonic to the fundamental. Therefore, a different dynamics is generated at either side of $\phi_0 = 0$.

Naturally, the dynamics of the beam evolution depends a great deal on both, the total and the relative input light intensities launched at each frequency. Figures 4-7 show the fundamental beams at $\xi = 10$, for different representative input light intensities with fixed topological charges of the phase-dislocation. In Figures 4 and 5 we set $m = 1$ and in Figures 6 and 7 we set $m = 2$. In Figures 4 and 6 the intensity of the fundamental beam is kept fixed whereas the intensity of the input second-harmonic beam varies, and viceversa for Figures 5 and 7. The plots show that, as expected on physical grounds, the precise pattern of output solitons is sensitive to the input intensities, mainly at the regime of lower input light intensities. For instance, in Figure 4(a) the input power is not high enough to allow the dynamical formation of two solitons by the splitting of the input beams, therefore the output pattern is clearly different than the output obtained in the conditions in Figures 4(b)-(d). Nevertheless, for our present purposes the main conclusion to be

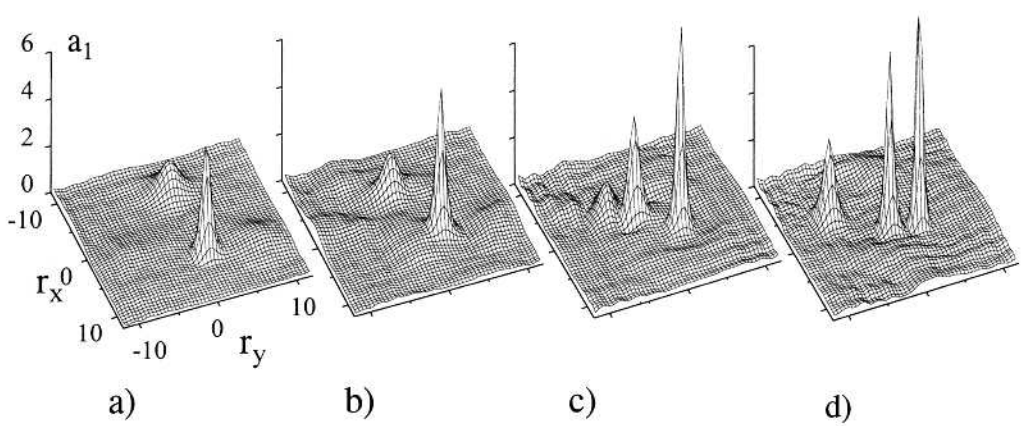

FIGURE 4. Fundamental beam after propagating up to $\xi = 10$ in a phase-matched configuration, for different values of the input light intensities with a fixed value of the phase dislocation of the second-harmonic input beam. In all cases $m = 1$ and $A = 3$. In (a): $B = 2$, in (b): $B = 3$, in (c): $B = 4$, and in (d): $B = 5$.

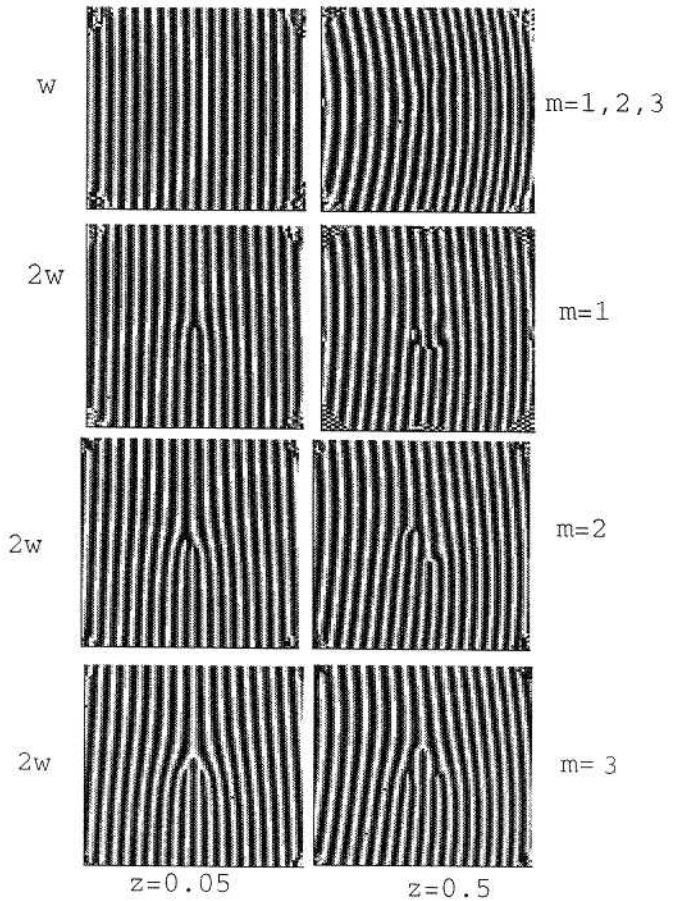

FIGURE 3. Interference fringes obtained by illuminating the fundamental and second harmonic beams with a plane wave tilted with relation to the propagation direction.

media: the addition of coherent fields induces splitting of a dislocation of charge m into $|m|$ single charge dislocations [12].

One salient point of Fig. 3 is that, for the specific conditions chosen, the number of solitons formed is equal to twice the charge of the vortex. This conclusion also holds for higher values of m than those shown here, provided that the input light intensity is high enough so that the $2m$ solitons can be formed dynamically by the process of beam splitting. This requires that the input light intensity is well above the threshold for the existence of $2m$ solitons, because the dynamics of the beam evolution produces dispersive waves that take energy away.

The self-splitting of the beams shown is due to the different dynamics experienced by the portions of the beams located at different azimuthal regions, as follows. Because of the helical phase-front of the second-harmonic input beam, the portions of the two interacting, fundamental and second-harmonic beams located in the different azimuthal positions experience a different phase relation and therefore undergo different dynamics. As a consequence, the beams split and, in those azimuthal regions where the particular initial dynamics favours the mutual trapping of the beams a soliton is formed. Otherwise, the corresponding portions of the beams tend to spread, and

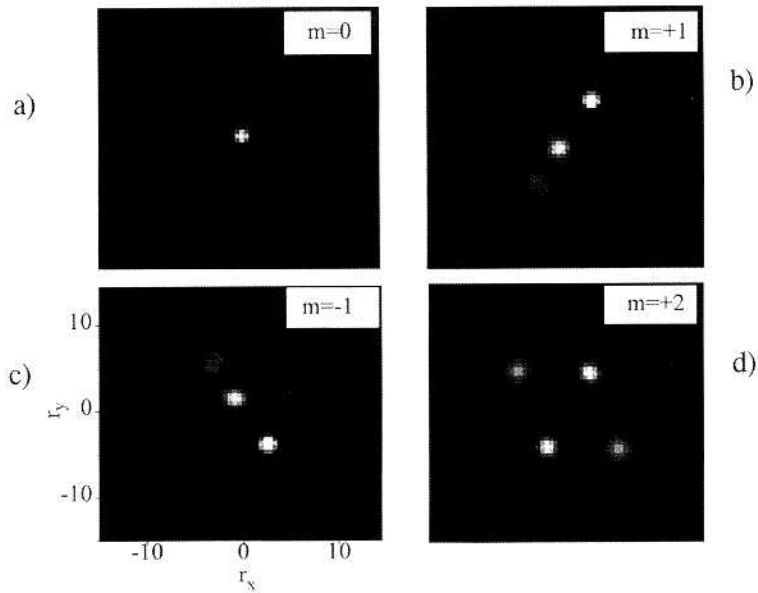

FIGURE 2. Fundamental beams after propagating up to $\xi = 12$, in a phase-matched configuration ($\beta = 0$), for different values of the charge of the phase dislocation of the second-harmonic input beam. The features shown are similar for the existing second-harmonic beam and have not been plotted. (a): $m = 0$, $A = 3$, $B = 5$; (b): $m = 1$, $A = 3$, $B = 4$; (c): $m = -1$, $A = 3$, $B = 4$; (d): $m = 2$, $A = 3$, $B = 2$. In all cases $\delta = 0$.

value of the various parameters involved, and in particular on the input light intensity, as we shall show and discuss shortly.

In the absence of the phase dislocation, the beams mutually trap and form one soliton as shown in Fig. 3(a). However, Figs. 3(b)-(d) show that when $m \neq 0$, the helical phase-front of the second-harmonic input produces the splitting of the beams into several solitons. We have verified that the fraction of the total Hamiltonian carried by each outgoing soliton amounts to a negative value, in agreement with the energy flow-Hamiltonian relation of the family of stationary soliton solutions [3]. The solitons emerge in different directions carrying different individual transverse momenta. Recall that the total transverse momentum $\vec{J}$ is conserved and that some fraction of it is in the form of radiation.

The total angular momentum L is also conserved. Therefore, either the pattern of output beams rotates during propagation or the relative phases of the several output solitons have to be different so that there is an azimuthally-asymmetric phase distribution. We observed that under most conditions studied, and in particular in all cases shown here, the latter is indeed the case. This fact might be partially responsible of the mutual repulsion that makes adjacent solitons to separate from each other.

The pattern of the interference fringes indicate no phase singularity in the fundamental beam and dislocations with a charge $m = 1$, 2 or 3 in the input second harmonic beam, depending on the charge of the initial vortex (Fig. 3). After some propagation distance a break-up of the defects with $m \neq 1$ into single-charge defects with the same sign is observed in the second harmonic beam while the fringes pattern for the fundamental beam remains practically unaltered. The break-up of the topological charge in the case $m > 1$ may be explained by a known effect in cubic nonlinear

For the right-hand-side of this equations to vanish in the presence of walk-off, the transverse momentum of the second-harmonic beam $\vec{\gamma}_2$ has to be parallel to $\vec{\delta}$, and such is the case when input light beams with azimuthal symmetry or with a phase-front tilt are considered[7,8]. Otherwise, as it is the situation that we study here, the total angular momentum is not conserved in the presence of Poynting vector walk-off.

To analyze the evolution of charge at the phase singularity (i.e., the value of m) in the beams of both frequencies, we studied the interference fringes arising by mixing the normalized calculated fields at a given distance ξ with a reference plane wave slightly tilted relative to the propagation axis. The tilt is towards the x axis. The resulting intensity from such an interference is now

$$I_{int} = \left| \frac{a_{1,2}(r\perp_x, r\perp_y)}{|a_{1,2}(r\perp_x, r\perp_y)|} + \exp\,(ik_x r\perp_x) \right|^2 , \tag{7}$$

where k_x is the spatial frequency of the tilted plane wave used as reference. The value of k_x is chosen for each field distribution to have good spatial resolution. Thus, a phase singularity appears as a dislocation, and a topological charge m is visually evaluated.

To monitor the formation and evolution of spatial solitons we calculated the Hamiltonian H, the components of transverse momentum J_x and J_y, and the angular momentum L_z relevant to a particular solitary wave by using the fields in the vicinity of the given solitary wave.

4. NUMERICAL EXPERIMENTS

To investigate the effect of the angular momentum associated with azimuthal symmetry breaking on the beam evolution, we performed series of numerical experiments solving eqs. (2) with a split-step Fourier algorithm and for a variety of input beam shapes and material conditions. Next we present the results obtained by taking Gaussian input beams with a phase dislocation nested in the second harmonic. We set,

$$\begin{aligned} a_1\,(\xi = 0, r\perp) &= A\,\exp(-r_\perp^2/w_1^2), \\ a_2\,(\xi = 0, r\perp) &= B r_\perp^{|m|} \exp(im\varphi)\,\exp(-r_\perp^2/w_2^2), \end{aligned} \tag{8}$$

where φ is the azimuthal angle in cylindrical coordinates, the integer m is the topological charge of the phase dislocation, and sgn(m) its chirality. In all the simulations presented in this paper we set $w_1 = w_2 = 2$. Notice that the input beams (8) carry the angular momentum $L = mI_2$, and that for a given amplitude B the power carried by the second-harmonic beam, I_2, is different for each value of $|m|$.

Our main goal is to elucidate the impact of the topological charge of the phase dislocation on the beam evolution, and we begin by examining the case of phase-matching ($\beta = 0$) in the absence of Poynting vector walk-off ($\delta = 0$). Figure 2 shows the summary of the output of a series of numerical experiments that display the main features of the beam evolution. The plots show the fundamental beams at ξ =12, for different values of the charge of the vortex in the second-harmonic input beam. The features of the second-harmonic fields are similar and thus not shown. The amplitudes of the beams A and B have been taken to be well above threshold for single soliton formation [3], and B has been chosen to yield similar values of I_2 regardless of the value of m. The results shown in Figure 2 are representative of the effects that occur over a range of input light conditions, but it is worth recalling that the precise pattern of output beams does depend on the

Gaussian beam. Figure 1(b) shows the principle of this transformation. A Hermite-Gaussian mode HG_{01} can be generated using a conventional laser if a crosswire is inserted into the laser cavity. To produce a $\pi/2$ phase shift a cylindrical lenses mode convertor may be used [16].

3. GOVERNING EQUATIONS

We consider cw light beams traveling in a medium with a large quadratic nonlinearity under conditions for Type I second-harmonic generation. In the slowly-varying envelope approximation, the beam evolution can be described by the reduced normalized equations [3].

$$\begin{aligned} i\,\frac{\partial a_1}{\partial \xi} - \frac{r}{2}\,\nabla_\perp^2 a_1 + a_1^* a_2 \exp(-i\beta\xi) = 0, \\ i\,\frac{\partial a_2}{\partial \xi} - \frac{\alpha}{2}\,\nabla_\perp^2 a_2 - i\delta\hat{\delta}\cdot\nabla_\perp a_2 + a_1^2 \exp(i\beta\xi) = 0, \end{aligned} \tag{2}$$

where a_1 and a_2 are the amplitudes of the fundamental and second-harmonic waves, $r = -1$, and $\alpha = k_1/k_2$. Here $k_{1,2}$ are the linear wavenumbers at both frequencies. In all cases $\alpha \cong -0.5$, so we set $\alpha = -0.5$. The parameter ß is given by $ß = k_1\eta^2\Delta k$, where $\Delta k = 2k_1 - k_2$, is the wavevector mismatch and η is a characteristic beam width. The parameter δ accounts for the Poynting vector beam walk-off that occurs in birefringent media when light propagation is not along the crystal optical axes, and is given by $\delta = k_1\eta\rho$, ρ being the walk-off angle. Poynting vector walk-off is absent in non-critical and typical quasi-phase-matching settings. Finally, in eqs. (1) the transverse coordinates are given in units of η, and the scaled propagation coordinate is $\xi = z/k_1\eta^2$. A detailed discussion of the impact of the above parameters on single soliton formation is given in References [3-8].

In the following we use three conserved quantities of the beam evolution, namely the beam power or energy flow, the Hamiltonian and the transverse beam momentum, which are respectively given by

$$I = I_1 + I_2 = \int \{|A_1|^2 + |A_2|^2\}\, dr\perp, \tag{3}$$

$$\begin{aligned} \mathcal{H} = -\frac{1}{2}\int \Big\{ r|\nabla\perp A_1|^2 + \frac{\alpha}{2}\,|\nabla\perp A_2|^2 - \beta|A_2|^2 + i\,\frac{\delta}{2}\,\hat{\delta}\cdot(A_2\nabla\perp A_2^* - A_2^*\nabla\perp A_2) \\ + (A_1^{*2}A_2 + A_1^2 A_2^*)\Big\}\, dr\perp, \end{aligned} \tag{4}$$

$$\vec{\mathcal{P}} = \vec{\mathcal{P}}_1 + \vec{\mathcal{P}}_2 = \frac{1}{4i}\int \left\{2(A_1^*\nabla\perp A_1 - A_1\nabla\perp A_1^*) + (A_2^*\nabla\perp A_2 - A_2\nabla\perp A_2^*)\right\} dr\perp, \tag{5}$$

where we have defined $A_1 = \alpha_1$, and $A_2 = \alpha_2 \exp(-i\beta\xi)$.

Because we consider input conditions without azimuthal symmetry, we study the evolution of the longitudinal component of the total angular momentum of the light beams given by $L = \int [\vec{r}\perp \mathrm{x}\, \vec{j}]_z\, dr\perp$, with $\vec{\mathcal{P}}$ being the transverse beam momentum density in expression (5). In the absence of Poynting vector walk-off, L is also a conserved quantity of the beam evolution. When walk-off is present, one readily finds that

$$\frac{dL}{d\xi} = \left[\vec{\delta}\,\mathrm{x}\,\vec{\mathcal{P}}_2\right]_z. \tag{6}$$

$$a(r\perp,z) = A\, r_{\perp}^{|m|} \exp(im\varphi)\, L_p^m\left(\frac{2|r\perp|^2}{w^2}\right)\exp\left(-\frac{|r\perp|^2}{w^2}\right) \qquad (1)$$

where $r\perp$ is the transverse radius-vector, L_m^p is the Laguerre polynomial, w is the beam width, A is the beam amplitude, $\varphi = \tan^{-1}(\mathrm{Im}(r\perp)/\mathrm{Re}(r\perp))$ is the azimuthal angle and m is the topological charge of the phase dislocation. We suppose in this study $m = 1$ or 2, and $p = 0$ or $p = 1$ so that the fields have cylindrical symmetry and have one or two nodes. The corresponding Laguerre polynomials are $L_0^1 = L_0^2 = 1$; $L_1^1 = 2 - \frac{2|r\perp|^2}{w^2}$; $L_1^2 = 3 - \frac{2|r\perp|^2}{w^2}$.

These beams can be generated experimentally by appropriate phase masks or by the transformation of Hermite-Gaussian modes with astigmatic optical components [15,16]. For example, when the pattern showed in Figure 1(a) is illuminated with coherent light, the first diffraction order produced has helical wave front with phase singularities that show up as defects in the fringes pattern of the interference between this beam and a non collinear plane wave.

Another way to generate Laguerre-Gaussian beams with phase singularities uses the Hermite-Gaussian output of a conventional laser and its transformation into the corresponding Laguerre-

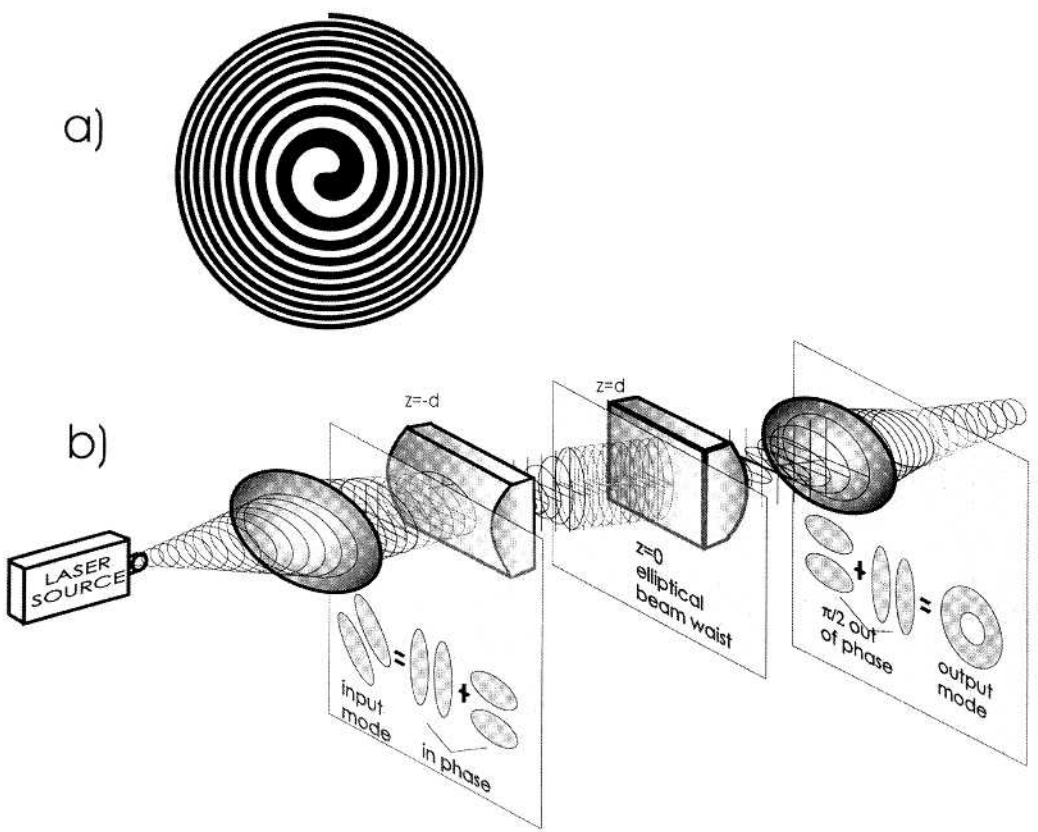

FIGURE 1. a) Computer-generated zone plates with $m = 1$. b) The cylindrical lens mode convertor. If the input $HG_{1,0}$ mode is oriented at 45° with respect to the cylinder axis of lens the mode is converted into the $LG^1{}_0$ mode. [See ref. 16 for details].

grant PB95-0768. We thank Ewan M. Wright for many ideas and suggestions about optical vortices and George I. Stegeman for useful discussions in the pursuing of this investigation. The numerical work has been carried out at the Centre de Computacio i Comunicacions de Catalunya.

REFERENCES

1. G.I. STEGEMAN, D.J. HAGAN, and L. TORNER: *Opt. Quantum Electron.*, (1996).
2. YU. N. KARAMZIN, and A.P. SUKHORUKOV: *Sov. Phys. JETP* **41**, 414 (1976).
3. L. TORNER, C.R. MENYUK, and G.I. STEGEMAN, J.: *Opt. Soc. Am. B* **12**, 889 (1995); L. Torner, and E.M. Wright: J. Opt. Soc. Am. B **13**, 864 (1996).
4. A.V. BURYAK, and Y.S. KIVSHAR: *Opt. Lett.* **19**, 1612 (1994); A.V. Buryak, Y. S. Kivshar, and V.V. Steblina, *Phys. Rev. A* **52**, 1670 (1995).
5. W.E. TORRUELLAS, Z. WANG, D.J. HAGAN, E.W. VANSTRYLAND, G.I. STEGEMAN, L. TORNER, and C.R. MENYUK: *Phys. Rev. Lett.* **74**, 5036 (1995).
6. R. SCHIEK, Y. BAEK, and G.I. STEGEMAN: *Phys. Rev. E* **53**, 1138 (1996).
7. L. TORNER, W.E. TORRUELLAS, G.I. STEGEMAN, and C.R. MENYUK: *Opt. Lett.* **20**, 1952 (1995); L. Torner, J.P. Torres, and C.R. Menyuk: *Opt. Lett.* **21**, 462 (1996).
8. W.E. TORRUELLAS, Z. WANG, L. TORNER, and G.I. STEGEMAN: *Opt. Lett.* **20**, 1949 (1995); W.E. Torruellas, G. Assanto, B.L. Lawrence, R.A. Fuerts, and G.I. Stegeman: Appl. Phys. Lett. **68**, 1449 (1996).
9. L. ALLEN, M.W. BEIJERSBERGEN, R.J. SPREEUW, and J.P. WOERDMAN: *Phys. Rev. A* **45**, 8185 (1992).
10. G.A. SWARTZLANDER, and C.T. LAW: *Phys. Rev. Lett.* **69**, 2503 (1992).
11. J.F. NYE, and M.V. BERRY: *Proc. R. Soc. London A* **336**, 165 (1974); G. Indebetouw: J. Mod. Opt. **40**, 73 (1993); F. S. Roux, J. Opt. Soc. Am. B **12**, 1215 (1995).
12. V.I. KRUGLOV, YU. A. LOGVIN, and V.M. VOLKOV: *J. Mod. Opt.* **39**, 2277 (1992); G.S. McDonald, K.S. Syed, and W.J. Firth: Opt. Commun. **94**, 469 (1992); I.V. Basistiy, V.YU. Bazhenov, M.S. Soskin, and M.V. Vasnetsov: Opt. Commun. **103**, 422 (1993); N.N. Rosanov, V.A. Smirnov, and N.V. Vyssotina: Chaos Solitons Fractals **4**, 1767 (1994).
13. B. LUTHER-DAVIES, R. POWLES, and V. TIKHONENKO: *Opt. Lett.* **19**, 1816 (1994).
14. V. TIKHONENKO, J. CHRISTOU, and B. LUTHER-DAVIES: *J. Opt. Soc. Am. B* **12**, 2046 (1995); V. Tikhonenko, and N. N. Akhmediev, Opt. Commun. **126**, 108 (1996).
15. N.R. HECKENBERG, R. MCDUFF, C.D. SMITH, and A.G. WHITE: *Opt. Lett.* **17**, 221 (1992).
16. M.W. BEIJERSBERGEN, R.P.C. COEWINKEL, M. KRISTENSEN, and J.P. WOERDMAN: *Opt. Commun.* **96**, 123 (1993), M. Padjett, J. Arlt, N. Simpson, and L. Allen: Am. J. Phys., **64**, 77 (1996).
17. S. TRILLO, and P. FERRO: *Opt. Lett.* **20**, 438 (1995); Phys. Rev. E **51**, 4994 (1995); A.A. Kanashov, and A.M. Rubenchik: Physica D 4, 122 (1981).
18. J.M. SOTO-CRESPO, D.R. HEATLEY, E.M. WRIGHT, and N.N. AKHMEDIEV: *Phys. Rev. A* **44**, 636 (1991); J.M. Soto-Crespo, E.M. Wright, and N.N. Akhmediev: Phys. Rev. A **45**, 3168 (1992).
19. W.H. PRESS, S.A. TEUKOLSKY, W.T. VETTERLING, B.T. FLANNERY: *Numerical Recipes in Fortran*, Second Edition, Cambridge University Press, 1992.